Plant Physiol. (1990) 93, 1610–1619
0032-0889/90/93/1610/10/$01.00/0

Received for publication November 20, 1989
Accepted May 3, 1990

# Wall Extensibility and Cell Hydraulic Conductivity Decrease in Enlarging Stem Tissues at Low Water Potentials[1]

**Hiroshi Nonami[2] and John S. Boyer***

*College of Marine Studies and College of Agriculture, University of Delaware, Lewes, Delaware 19958*

## ABSTRACT

**Measurements with a guillotine psychrometer (H Nonami, JS Boyer [1990] Plant Physiol 94: 1601–1609) indicate that the inhibition of stem growth at low water potentials (low $\psi_w$) is accompanied by decreases in cell wall extensibility and tissue hydraulic conductance to water that eventually limit growth rate in soybean (*Glycine max* L. Merr.). To check this conclusion, we measured cell wall properties and cell hydraulic conductivities with independent techniques in soybean seedlings grown and treated the same way, *i.e.* grown in the dark and exposed to low $\psi_w$ by transplanting dark grown seedlings to vermiculite of low water content. Wall properties were measured with an extensiometer modified for intact plants, and conductances were measured with a cell pressure probe in intact plants. Theory was developed to relate the wall measurements to those with the psychrometer. In the elongation zone, the plastic deformability of the walls decreased when measured with the extensiometer while growth was inhibited at low $\psi_w$. It increased during a modest growth recovery. This behavior was the same as that for the wall extensibility observed previously with the psychrometer. Tissue that was killed before measurement with the extensiometer also showed a similar response, indicating that changes in wall extensibility represented changes in wall physical properties and not rates of wall biosynthesis. The elastic compliance (reciprocal of bulk elastic modulus) did not change in the elongating or mature tissue. The hydraulic conductivity of cortical cells decreased in the elongating tissue and increased slightly during growth recovery in a response similar to that observed with the psychrometer. We conclude that the plastic properties of the cell walls and the conductance of the cells to water were decreased at low $\psi_w$ but that the elastic properties of the walls were of little consequence in this response.**

Cell enlargement is the first physiological process to be affected when the soil water supply begins to be depleted (3). We studied the mechanisms affecting enlargement under these conditions by growing dark-grown seedlings in vermiculite of low water content (see Nonami and Boyer [27] and references cited therein). We showed that stem elongation decreased soon after the exposure to limited water and that the water potential gradient bringing water into the elongating cells was the first growth parameter to decrease to growth-limiting levels. With the exception of a few cells close to the xylem, the turgor remained virtually constant in the elongating cells throughout the measurements (26, 27). Eventually, cell wall properties were changed at low $\psi_w$,[3] especially the wall extensibility and the tissue conductance for water (27). Subsequently, the gradient reformed but the wall extensibility and hydraulic conductance remained low and ultimately became the main factors limiting growth.

This result indicates that plant metabolism responded to early events in the growth inhibition. Among the metabolic changes that were detected were lower polyribosomal contents (21), higher abscisic acid contents (2), higher extractable amounts of cell wall proteins (6) and lower rates of wall acidification (35). Some of the metabolic changes (2, 6, 21) were initiated as the gradient changed and became large when the extensibility and conductance changed. Therefore, the kinetics are consistent with a role for altered metabolism in the response of the walls and membranes.

The changes in wall extensibility and hydraulic conductance (27) were determined from the forces that enlarged the cells, *i.e.* the water potential ($\psi_w$), turgor ($\psi_p$), and osmotic potential ($\psi_s$) measured with a guillotine psychrometer (4). Because the method is new and the kinetics of the wall and membrane changes are crucial to the hypothesis of an eventual metabolic control of growth rate, we sought independent methods of measuring wall extensibility and hydraulic conductance directly. To be strictly comparable to the psychrometer experiment, which involved intact plants, the methods also had to use intact plants. No method is presently available for studying wall properties in this way. Therefore, we modified an extensiometer method (19, 20) so that it could be used with intact plants, and we used a miniature pressure probe (18) to measure cell hydraulic conductivities in intact plants. These measurements are reported here for comparison with those of the psychrometer (27).

[1] Supported by Department of Energy grant DE-FG02–87ER13776 and a grant from E. I. duPont de Nemours and Company to J.S.B.

[2] Present address: Department of Bio-mechanical Systems, College of Agriculture, Ehime University, Tarumi, Matsuyama 790, Japan.

[3] Abbreviations: $\psi_w$ = water potential (MPa); $\psi_p$ = turgor (MPa); $\psi_s$ = osmotic potential (MPa); $G$ = relative enlargement rate ($s^{-1}$); $m$ = extensibility ($s^{-1} \cdot MPa^{-1}$); $Y$ = yield threshold turgor (MPa); $\gamma$ = strain (relative change in dimensions, unitless); $\sigma$ = stress (applied force per unit area or pressure, $N \cdot m^{-2}$ or MPa); $E$ = elastic compliance ($m^2 \cdot N^{-1}$ or $MPa^{-1}$, the inverse of Young's modulus of elasticity); $M$ = plastic deformability ($m^2 \cdot N^{-1} \cdot s^{-1}$ or $s^{-1} \cdot MPa^{-1}$); $X$, $Y$, $Z$ = lengths in the $X$, $Y$, or $Z$ directions (m); $F$ = force ($N$); $A$ = cross sectional area ($m^2$); $V$ = volume ($m^3$); $\nu$ = Poisson's ratio (ratio of relative thinning to relative lengthening when material is stretched lengthwise, dimensionless); $B$ = bulk compliance ($m^2 \cdot N^{-1}$ or $MPa^{-1}$, the inverse of the bulk modulus of elasticity $\epsilon$); $L_p$ = hydraulic conductivity for water ($m \cdot s^{-1} \cdot MPa^{-1}$); $T_{1/2}$ = half time (s); $A_s$ = surface area of cell ($m^2$).

## THEORY

To make the comparison for cell walls, it is necessary to relate psychrometer data involving three-dimensional forces within cells and extensiometer data involving one-dimensional forces applied from outside. For simplicity, we consider plant tissues to consist of a continuous viscoelastic polymer (cell walls) containing extremely small compartments (cells) with bounding membranes. Water moves throughout the polymer in the walls and cells. Internal pressures exert forces in three directions inside the cells and, for experimental purposes, force is applied in one direction to the entire tissue.

### Physical Properties of Cell Walls

As in Nonami and Boyer (27), wall extensibility is defined operationally as a coefficient m that indicates the relative enlargement rate $G$ ($s^{-1}$) when the growth-active turgor ($\psi_p - Y$) is known in intact plants:

$$G = m(\psi_p - Y) \quad (1)$$

where $m$ has units of $s^{-1} \cdot MPa^{-1}$, $\psi_p$ is the turgor and $Y$ is the yield threshold turgor (MPa). Wall extensibility is determined by the physical properties of the existing wall and any additional effects caused by the synthesis of new wall. Because the extensibility is defined in terms of turgor, wall extension must be analyzed three-dimensionally.

On the other hand, an external force applied in one direction to plant tissues will cause a deformation in proportion to the force if the force is small (1, 36). If the walls consist of mixtures of ideal elastic (Hookian) and ideal nonelastic viscous materials (Newtonian), the Boltzmann superposition principle (1, 36) indicates that the deformation can be split linearly into an elastic component and a plastic component. Energy used for elastic deformation is conserved whereas energy for plastic deformation partly rearranges the molecules and partly is dissipated as heat.

Elastic deformation is instantaneous, reversible, and independent of time:

$$d\gamma = E(d\sigma) \quad (2)$$

where $\gamma$ is the strain (relative change in dimensions, unitless), $\sigma$ is the stress (applied force per unit area, or pressure, $N \cdot m^{-2}$ or MPa), and $E$ is the elastic compliance ($m^2 \cdot N^{-1}$ or $MPa^{-1}$, the inverse of Young's modulus of elasticity).

Plastic deformation is not instantaneous nor reversible, and it occurs continuously at a rate in proportion to the stress:

$$d\gamma/dt = M\sigma \quad (3)$$

where $M$ is the plastic deformability ($m^2 \cdot N^{-1} \cdot s^{-1}$ or $s^{-1} \cdot MPa^{-1}$).

The superposition principle allows the sum of Equations 2 and 3 to be obtained after differentiating Equation 2 by time to give the governing equation (1, 36):

$$d\gamma/dt = E(d\sigma/dt) + M\sigma. \quad (4)$$

Equation 4 shows that there will be an elastic deformation only when the force changes but a plastic deformation that progresses as long as force is applied. This concept is useful for distinguishing elastic deformation from plastic deformation while growth is occurring in the intact plant.

### Elastic Component

A plant stem to which a force is applied in one direction parallel to the long axis ($z$-direction) will stretch instantaneously. Before significant time elapses, plastic deformation is zero so that Equation 4 reduces to Equation 2 stated as:

$$dZ/Z = Ed\sigma = EdF/A \quad (5)$$

where $Z$ is the length in the $z$-direction, $F$ is the force, and $A$ is the cross-sectional area of the tissue.

On the other hand, because cell turgor stretches the wall three-dimensionally, causing a fractional volume change $dV/V$, the volume change is related to the length change for isotropic materials by (1, 16, 36):

$$dV/V = 3(1 - 2\nu)dZ/Z \quad (6)$$

where $\nu$ is Poisson's ratio, a unitless term that corrects unidirectional dimensions for contributions from other directions and is defined by: $dX/X = dY/Y = -\nu\, dZ/Z$. Poisson's ratio varies between 0 and 0.5. For nonisotropic materials, the relation $3(1 - 2\nu)$ must be modified to a more complex form. However, if $\nu$ approaches 0 or 0.5, the complex forms are approximated by $3(1 - 2\nu)$ and Equation 6 holds for both isotropic and nonisotropic materials (see examples in Feynman *et al.* [16]).

Substituting $dZ/Z$ from Equation 6 into Equation 5 gives:

$$dV/V = 3(1 - 2\nu)Ed\psi_p = B(d\psi_p) \quad (7)$$

where $\psi_p$ is $F/A$ operating in three dimensions (*e.g.* the turgor) and:

$$B = 3(1 - 2\nu)E. \quad (8)$$

$B$ is the bulk compliance and has units of $m^2 \cdot N^{-1}$ or $MPa^{-1}$ (36), *i.e.* $B$ is the inverse of the bulk modulus of elasticity $\epsilon$. From Equation 7, $B$ can be measured with a pressure probe and, from Equation 5, $E$ can be measured with an extensiometer. Poisson's ratio, $\nu$, can be measured from changes in dimension. Thus, Equation 8 allows three-dimensional and one-dimensional elasticity measurements to be compared.

### Plastic Component

Many materials deform irreversibly only when the applied stress exceeds a minimum necessary for molecular rearrangement. The minimum is termed the yield threshold and is observed in cell walls that, under a constant stress exceeding the threshold, deform continuously and irreversibly, resulting in cell enlargement. The deformation appears to be linear (Newtonian) with the applied stress (9, 17, 22, 30) and thus can be considered ideal. Over significant time with constant stress, $d\sigma/dt$ is zero (Eq. 4) and the elastic component does not contribute. Thus, for a stress applied in one dimension, Equation 4 becomes:

$$(dZ/dt)(1/Z) = M(F/A). \quad (9)$$

In a stem with cross-sectional area A that is essentially con-

stant, one-dimensional and three-dimensional strains are related by $(dZ/dt)(1/Z) = (AdZ/dt)(1/AZ) = (dV/dt)(1/V) = G$. Also, because $F/A$ operating in three dimensions is the pressure, the $F/A$ for plastic deformation in three dimensions is $(\psi_p - Y)$. The plastic deformability $M$ measured in one dimension (Eq. 9) is then the extensibility $m$ measured in three dimensions (Eq. 1):

$$(dZ/dt)(1/Z)/(F/A) = G/(\psi_p - Y) = M = m. \quad (10)$$

From Equation. 1, $m$ can be evaluated with a psychrometer and from Equation. 9, $M$ can be measured with an extensiometer, and Equation 10 allows these three-dimensional and one-dimensional measurements to be compared. Although this conclusion can be complicated by the synthesis of new wall material, in principle the effect of synthesis can be tested by determining $M$ when the tissue is synthesizing new wall and when it is not.

## MATERIALS AND METHODS

### Plant Material

Soybean (*Glycine max* [L.] Merr. cv Williams) seedlings were grown as previously described (27). Briefly, the seeds were disinfected in a 1% solution of NaOCl for 5 min, rinsed with flowing water for 1 h, sown in vermiculite with adequate water (5.0 mL of 0.1 mM $CaCl_2$/g of vermiculite, *i.e.* $\psi_w$ of −0.01 MPa), and grown at 29 ± 0.5°C and saturating humidity in darkness. After 55 to 60 h, they were transplanted to a 200-mL beaker containing either similar vermiculite (1× treatment) or water-deficient vermiculite (1/8 the amount of water). The vermiculite $\psi_w$ was −0.28 ± 0.02 MPa when measured with an isopiestic thermocouple psychrometer (5) as described elsewhere (26). After transplanting, the seedlings were returned to the growth environment. All seedling manipulations were done in the growth environment under a green safelight.

### Extension Measurements

Soybean stems (hypocotyls) were subjected to small extensions by hanging various weights on a nylon thread and leading the thread over a pulley to the stem where it was connected to the hypocotyl hook of the intact plant. Extension occurred upward as the force was applied and was measured with a radial displacement transducer whose arm was attached adjacent to the thread attachment. A rigid reference bar was attached at a position immediately below the elongating region. The length of this region was estimated from the plant height according to Figure 1 because the elongating zone lengthened as the plant became older. The diameter of the stem and the distance between the attachments were measured accurately with a caliper. Extension measurements were made in the mature zone by attaching the transducer arm and the reference bar near the base of the stem. The body of the transducer was mounted in the barrel of a microscope so that calibration could be carried out at any time without disturbing the plant materials. Seedlings could grow without restriction in the vermiculite while attached to the transducer. The experiments were conducted in the growth environment with the entire apparatus and seedling in a dark box having saturating humidity.

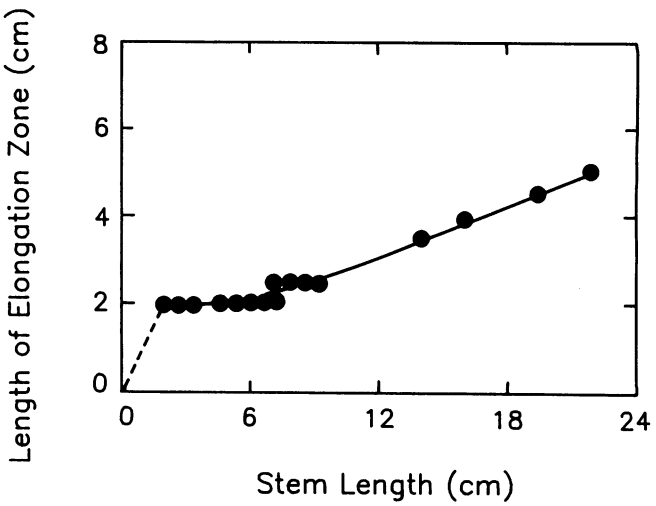


**Figure 1.** Relationship between the length of the stem elongating region and the total length of the stems of soybean seedlings. Stems were marked in 5-mm intervals with India ink and the lengths were determined after 3 h. *Dashed line* indicates time during early germination when stem consisted entirely of elongating tissue.

Small extensions were also generated in the elongating region after killing the tissue. The zone of elongation of an intact seedling was attached to the transducer as described above and, after growth was steady, liquid dichlorodifluoromethane (Fisher Scientific) was sprayed directly on the zone of elongation for a few seconds, as in Kutschera and Schopfer (19, 20). Freezing took place immediately and, after thawing, force was applied to the killed tissue in the same way as in the living tissue.

In living and killed tissue, changes in stem diameter were measured with a microscope before, during and after force application to calculate Poisson's ratio.

In one experiment, the epidermis-hypodermis complex was excised from the elongating region and force was applied to the cortex-stele. The excision was done by first removing the apical hook from an elongating seedling, inserting a sharpened-stainless steel capillary (o.d. = 1.47 mm, i.d. = 1.19 mm; Small Parts Inc.) perpendicularly to the cut end along the stem axis for the length of the elongating region, and cutting away the tissue outside of the capillary. Tissue inside the capillary was pushed out with a 1-mm diameter glass rod and immediately coated with petrolatum. The cut end was attached to the transducer and connected to the loading thread with a small clip. After the growth rate of the tissue became stable, although it was extremely low, stress-strain relations were determined as above.

### Turgor, Bulk Compliance, and Hydraulic Conductivity

Cell turgor was measured in the cortical cells with a pressure probe as described previously (28). It was necessary to coat the stems with petrolatum before measurement to prevent local dehydration under the green light used with the pressure probe (28). The hydraulic conductivity of the cells was meas-

ured by injecting a small amount of cell solution with the probe and determining the half time ($T_{1/2}$) for water to move out of or into the cell from the surroundings. The water movement was determined from the dimensions of the probe tip and the movement of the meniscus between the cell solution and the oil in the tip (18). The hydraulic conductivity of the cell ($L_p$, $m \cdot s^{-1} \cdot MPa^{-1}$) was calculated from $T_{1/2}$ (s) according to:

$$L_p = (VB \ln 2)/(A_s T_{1/2}(1 - \psi_s B)) \quad (11)$$

where $V$ is the cell volume ($m^3$), $B$ is the bulk compliance ($MPa^{-1}$), $A_s$ is the surface area of the cell ($m^2$), and $\psi_s$ is the osmotic potential (MPa). Cell $A_s$ and $V$ were calculated from cell diameters and lengths measured under a microscope with fresh sections. The $\psi_s$ was obtained from isopiestic psychrometer measurements (5) from previously published values (27, 28). The bulk elastic compliance $B$ was measured in the cortical cells by instantaneously injecting a small volume of cell solution with the pressure probe and briefly recording the change in turgor. The cell was quickly returned to the original volume by removing solution with the probe so that plastic deformation and water exchange were avoided. The $B$ was calculated according to Equation 7: $(dV/V)/(d\psi_p) = B$.

## RESULTS

The determination of the elastic and plastic properties of the wall required the length of the zone of elongation to be known with accuracy (Eqs. 5–10). Marking the stem at 5-mm intervals and measuring the length between marks after 3 h showed that the zone lengthened as the stem grew (Fig. 1). At low $\psi_w$, this relationship was unchanged (H. Nonami, J. S. Boyer, unpublished data, and see Meyer and Boyer [24]). In the succeeding experiments, the measurements with the transducer and all calculations were made for the length of the elongating zone prevailing at the time, judged from the total stem length.

### Elastic Compliance and Plastic Deformability

We tested the effects of applying a one-dimensional force to the stem of an intact soybean seedling that grew during the measurement. Application of an upward force caused extension of the stem, and removal of the force caused contraction of the stem (Fig. 2). If significant time elapsed, extension was always greater than contraction, as expected if extension contained an elastic component plus a plastic deformation but contraction contained only an elastic component. Thus, the plastic component could be measured from the difference between the extension and the contraction when a period of time had elapsed between them.

We applied various extending forces to a maximum of $0.343N$ to stems that averaged $1.1 \times 10^{-3}$ $m$ in radius. This was equivalent to about $0.9 \times 10^5$ $N \cdot m^{-2}$ of stem cross-section or about 20% of the force exerted in the lengthwise direction by the turgor of $4.5 \times 10^5 N \cdot m^{-2} = 0.45$ MPa (see turgor in Fig. 7B). On average, the elongating region of the stems increased to 1.0048× their original length $Z$ and the diameter decreased to 0.998× the original diameter $Y$ when this extending force was applied instantaneously. This gave a Poisson's ratio $\nu = -(dY/Y)/(dZ/Z) = -(-0.002/1)/(0.0048/1) = 0.42 \pm 0.02$ (95% confidence interval) for the living tissue, which was close enough to 0.5 that any nonideal elastic behavior was ignored.

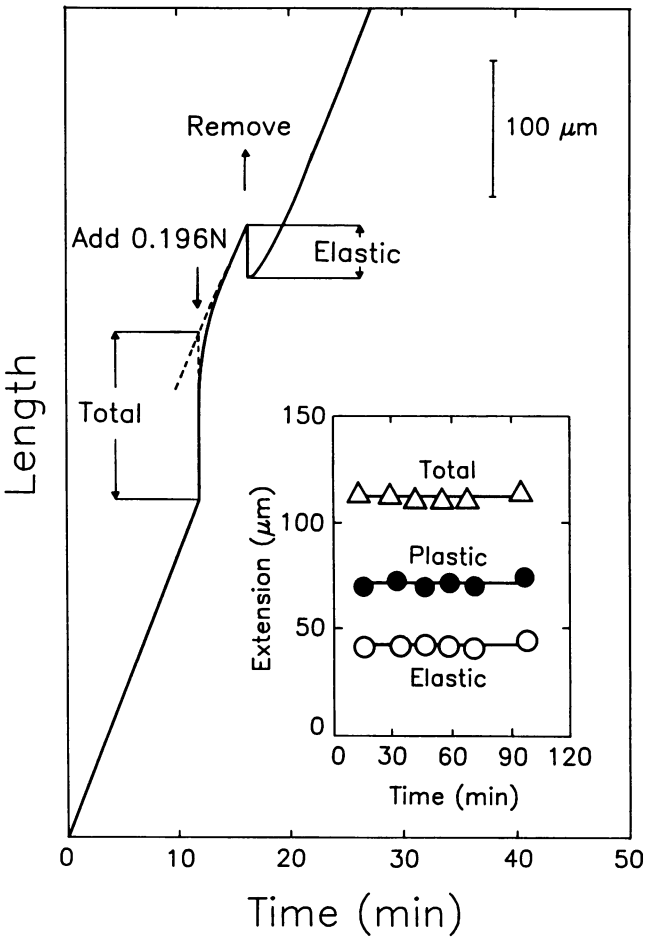


**Figure 2.** Extension and contraction induced by application and removal of a force of 0.196 $N$ (equivalent to 20 g) to a stem of an intact soybean seedling having a growth rate of 0.47 $\mu m \cdot s^{-1}$. The force was applied to the elongating region at the *downward arrow* and removed at the *upward arrow*. Plastic extension was defined as the difference between the total extension (extrapolated at *downward arrow*) and the elastic contraction (*upward arrow*). The dashed line having a slope shows the growth rate before force application and, when extrapolated to the time of force application, gives the total extension that occurred in initial 3 to 6 min after force was applied (in this case 3.2 min). *Inset*: repeatability of total, plastic, and elastic extension during repetitive force application (0.196$N$) and removal from the same elongating region.

The lengthwise changes required about 3 to 6 min to achieve a new steady slope after the force was applied (Fig. 2). Initially, the growth rate was not markedly different from that before the stress was applied but if the force was maintained for longer than about 10 min, the elongation rate accelerated (e.g., see initial part of Fig. 5A), suggesting that the cells were acclimating to the new stress. To avoid possible changes in wall properties, the measurements were completed

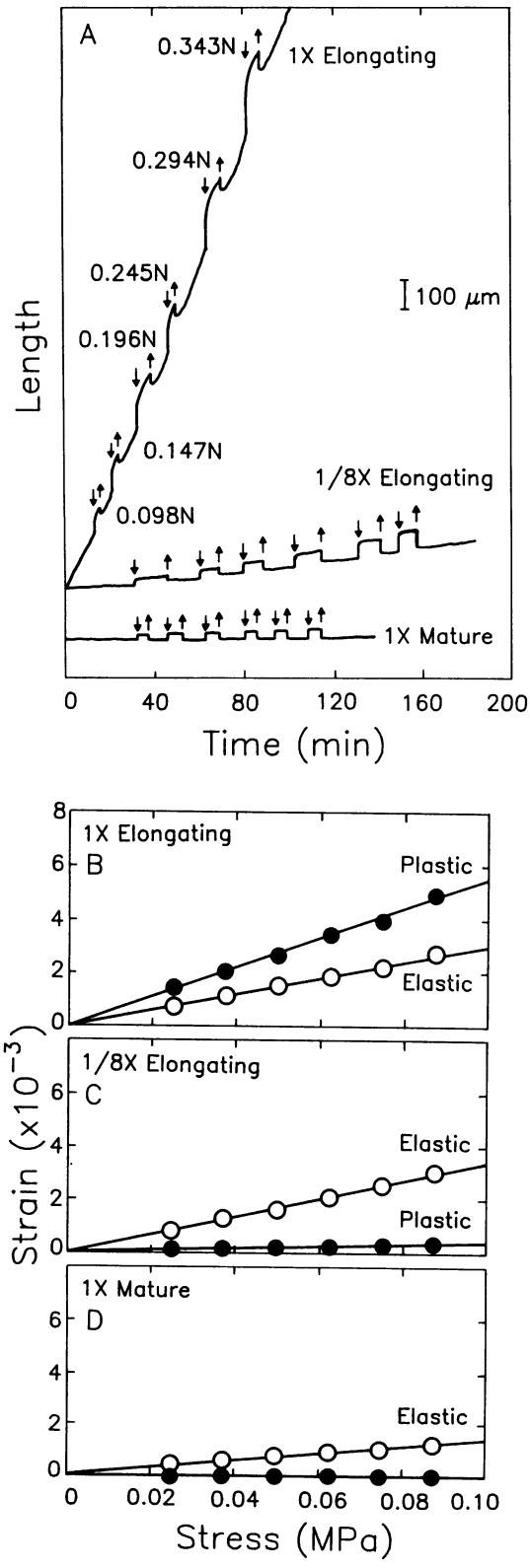


**Figure 3.** (A) Extension and contraction induced by sequential force application and removal (*i.e.* forces of 0.098*N*, 0.147*N*, 0.196*N*, 0.245*N*, 0.294*N*, and 0.343 *N*) from the stem of intact soybean seedlings growing in 1× vermiculite or 1/8× vermiculite. Measurements were made in the elongating region (1× elongating and 1/8× elongating) or in the mature region (1× mature). The forces were applied at *downward arrows* and removed at *upward arrows*. In (A), 1× Elongating was measured while the stem grew at 0.47 $\mu m \cdot s^{-1}$ in the 17th h after transplanting; 1/8× Elongating was measured while the stem grew at 0.01 $\mu m \cdot s^{-1}$ in the 22nd h after transplanting; and 1× Mature was measured while the stem grew rapidly but the mature region showed zero elongation 21 h after transplanting. (B, C, and D) Stress-strain relations determined from the length changes in (A). Stress (MPa) was calculated from weight (*N*) per unit cross-sectional area of stem calculated from stem diameter measured with a caliper (1 MPa = $10^6 N \cdot m^{-2}$). (○) = elastic component; (●) = plastic component.

in the initial 3 to 6 min. We defined the plastic component of the total extension to be the amount of length increase between the time immediately after force application (immediately after elastic extension) and the time to reach a new steady rate (Fig. 2). The endogenous growth rate was eliminated from the measurement by extrapolating to the time of force application a line having the same slope as before the force application (as in Fig. 2).

Elastic extension was defined as the length of contraction within 30 s after removal of the force (Fig. 2). Because the growth of the plant resumed within 1 to 3 min after the force was removed (Fig. 2), stress relaxation was very rapid in intact plants, confirming earlier observations (4, 23).

Stress extension and relaxation could be repeated in the same plant without change (*inset*, Fig. 2). Because the tissue was growing, cell turgor maintained the stress above the yield threshold. Therefore, when various forces were applied to the same tissue (Fig. 3A), the stress-strain relations were linear for both the elastic and plastic components (Fig. 3, B–D) and there was no evidence of a yield threshold, *i.e.*, the relationship for the plastic component extrapolated to zero when the added stress was zero. In the elongating region of rapidly growing stems, the plastic component was larger than the elastic component (Fig. 3B). In stems growing slowly because of exposure of the plants to low $\psi_w$, the plastic component was smaller than the elastic component (Fig. 3C). The elastic component was unaffected by the growth inhibition (*cf.* Fig. 3, B and C). In the mature region, the elastic component was small and there was no plastic component (Fig. 3D).

An average plastic deformability could be obtained from plots like Figure 3 by determining the slope of the stress-strain relations $(dZ/Z)/(F/A)$ and dividing by the average time to reach the new steady state $(1/dt)$ according to Equation 9: $(1/dt)(dZ/Z)/(F/A) = M$. When we used this approach to follow changes in the plastic deformability of seedlings exposed to low $\psi_w$, the deformability remained high in the controls but decreased during exposure of the seedlings to low $\psi_w$, then increased to an intermediate level (Fig. 4A). The initial decrease was apparent by 5 h after transplanting. These changes took place at about the same time as the extensibility changes measured in the guillotine psychrometer (27) and were numerically similar (27), confirming that the plastic deformability was equal to the wall extensibility. In the mature tissue, the plastic deformability was zero (Fig. 4C).

An average elastic compliance $E$ was measured similarly

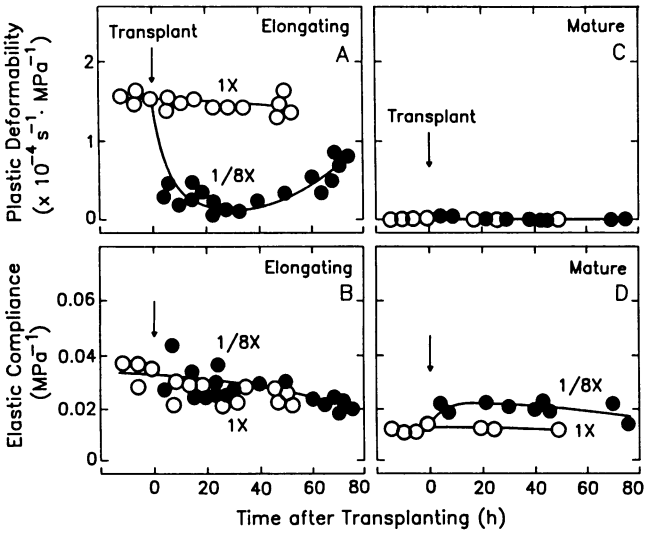


**Figure 4.** Plastic deformability (A and C) and elastic compliance (B and D) measured in the elongating zone (A and B) and mature zone (C and D) of stems of soybean seedlings transplanted to well-watered vermiculite (1×) or water-deficient vermiculite (1/8X). Measurements were made with extensiometer according to Figures 1 to 3. (○) represent 1× plants and (●) represent 1/8× plants. Each point is an individual measurement.

from the slopes of the stress-strain relations according to Equation 5: $(dZ/Z)/(F/A) = E$. The compliance was the same in the controls and treated plants (Fig. 4B). In the mature zone, the compliance of growth-inhibited plants increased slightly over the control (Fig. 4D).

We explored the contribution of cell wall biosynthesis to wall extensibility by repeating these measurements in tissue killed by freezing and thawing. The frozen-thawed tissue was considerably shorter than the same tissue when alive, and it lengthened and narrowed an average 1.045× and 0.973×, respectively, relative to the unstressed dimensions when a force of 0.343*N* was applied (Fig. 5). This gave a Poisson's ratio of 0.60 ± 0.04 (95% confidence interval), which is outside the theoretical range for elastic materials. However, we noted that cell solution sometimes leaked out and appeared on the stem surface when the force was applied, which could lead to nonideal behavior. This was not observed in the living tissue. Because the frozen/thawed tissue behaved ideally in every other way, we assumed that the superposition principle continued to hold.

The elastic extension and narrowing of the stem were rapidly reversible and repeatable in each frozen-thawed plant (Fig. 5, A and C). However, plastic deformation was observed mostly during the first extension after freeze-thawing (Fig. 5, A and B). Therefore, different seedlings were used for each force application to construct stress-strain relations as in Figure 3, B–D. The relationships were linear (data not shown).

The plastic deformability obtained in the elongating region of killed tissue decreased during exposure of the plants to low $\psi_w$ but increased after 40 h, and had values similar to those in the living tissue (*cf.* Figs. 4A and 6A). The elastic compliance of frozen-thawed tissue also behaved in a fashion similar

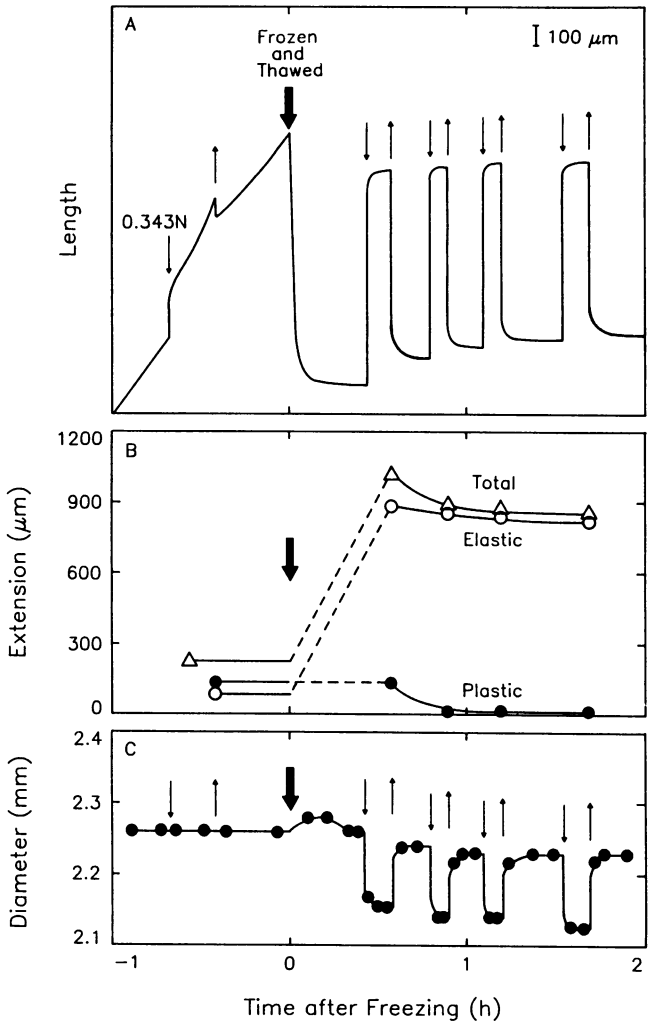


**Figure 5.** (A) Extension and contraction curves caused by an external force applied to the elongating region of the stem of an actively growing soybean seedling before and after freeze/thawing. The force (0.343*N*) was applied to the living stem at the downward and upward arrows on the left. The stem was frozen instantaneously by spraying liquid dichlorodifluoromethane at the *heavy arrow*. After thawing, the same force was applied repeatedly to the killed stem. Note the acceleration in rate of growth 10 min after the first force application (before freeze/thawing), indicating acclimation to new force. All measurements of plastic extension were made before this acceleration, as in Figure 2. (B) Total, elastic, and plastic extension determined from (A) according to Figures 1 to 3. *Dashed lines* indicate time of freeze-thawing. (C) Typical changes of stem diameter observed under the microscope during extension and contraction caused by the force application in (A). Stems were 9 cm long with an elongating region 2.5 cm long.

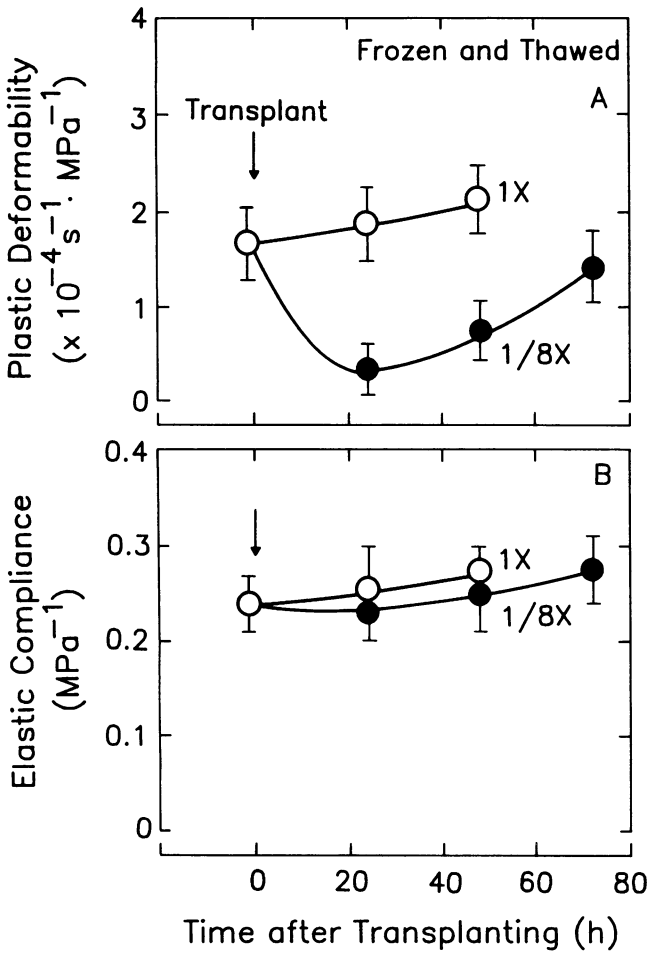


**Figure 6.** Plastic deformability (A) and elastic compliance (B) of the elongating region of frozen and thawed soybean stems of otherwise intact seedlings. Measurements were made according to Figures 1 to 3 and Figure 5 using an extensiometer. (○) represent plants grown in 1× vermiculite and (●) represent plants grown in 1/8× vermiculite. *Vertical bars* indicate 95% confidence intervals (Student's *t*-distribution).

to that of living tissue, showing no change at low $\psi_w$ (*cf.* Figs. 4B and 6B). However, the compliance was about 10 times larger than in living tissue. This probably was caused by the loss of tension on the epidermal-hypodermal tissues induced by turgor loss when the tissue was killed. Removal of the epidermis-hypodermis from living elongating tissue caused the elastic compliance to increase from 0.035 ± 0.005 $MPa^{-1}$ in the intact tissue to 0.29 ± 0.02 $MPa^{-1}$ in the tissue with epidermis/hypodermis removed indicating that, without the epidermis/hypodermis, the elastic compliance of living tissue was similar to that for the killed but otherwise intact tissue.

### Bulk Compliance and Cell Turgor

We wished to test whether the tissue elasticity could be confirmed by an independent technique. By determining the bulk compliance of the living tissue $3(1 - 2\nu)E = B$ using $\nu$ and $E$ measured as above, we could compare $B$ with measurements from individual cortical cells $(dV/V)/d\psi_p = B$ using the pressure probe (see Eqs. 7 and 8). The pressure probe measurements were made in the cortical tissue at a depth of 70 to 300 μm in the elongating tissue and a depth of 100 to 350 μm in the mature tissue. From the depth of penetration of the probe, we could estimate the average size of the cells at each depth from fresh sections of tissue. These were used with the pressures at that depth in the calculations of $B$. Cell diameters ranged between 35 and 65 μm in the elongating region and 42 to 77 μm in the mature region. Cell lengths ranged between 208 and 260 μm in the elongating region and 338 to 370 μm in the mature region. Cell volumes calculated from these dimensions were 331 to 511 pL in the elongating region and 718 to 1424 pL in the mature region.

In the elongating tissue, the average $B$ of the cortical cells measured with the pressure probe (0.35 $MPa^{-1}$, Fig. 7A) was moderately greater than $B$ for the whole tissue measured with the extensiometer (0.15 $MPa^{-1}$, calculated from Fig. 4B and Poisson's ratio) perhaps reflecting a greater constraining effect of the epidermis/hypodermis on the tissue than on the individual cells. The $B$ at the cell level (Fig. 7A) did not change when the seedlings were exposed to low $\psi_w$, confirming the similar behavior of the elastic compliance at the tissue level (Fig. 4B). The turgor was about 0.45 MPa and constant (Fig. 7B) in agreement with the psychrometer results (26, 27). In the mature region, the compliance increased immediately after the plant was transplanted to 1/8× vermiculite (Fig. 7C) probably because turgor decreased (Fig. 7D) which released some of the strain on the cell walls. The turgor decreased because water was withdrawn from the mature tissue to feed the slow growth in the elongating zone (R. Matyssek, A.-C. Tang, J. S. Boyer, unpublished data). After 40 h, the compliance and turgor returned to the original level. This turgor dependence of the compliance is similar to that reported by others (*e.g.* Steudle *et al.* [34]).

### Hydraulic Conductivity and Hydraulic Conductance

Using the above dimensions, the surface area of the cells ranged between 3.03 to 4.48 × $10^{-8}$ $m^2$ in the elongating region and 5.66 to 8.38 × $10^{-8}$ $m^2$ in the mature region at the depths where the pressure probe measurements were made. To calculate $L_p$ from Equation 11, we used $B$ from Figure 7A and $\psi_s$ from Nonami and Boyer (27) for elongating tissue and from Nonami *et al.* (28) for mature tissue. The hydraulic conductivity of cortical cells in the elongating region decreased after exposing the seedlings to low $\psi_w$ and increased slightly about 40 h later (Fig. 8A). This behavior at the cellular level is similar to that at the tissue level measured with the psychrometer (27) although the numerical values differ. In the mature region, the hydraulic conductivity showed the inverse pattern, increasing initially and decreasing gradually afterward (Fig. 8B).

## DISCUSSION

In a companion study (27), we determined the wall extensibility and hydraulic conductance of soybean stems using psychrometer measurements of tissue water status and observed that these parameters decreased a few hours after the

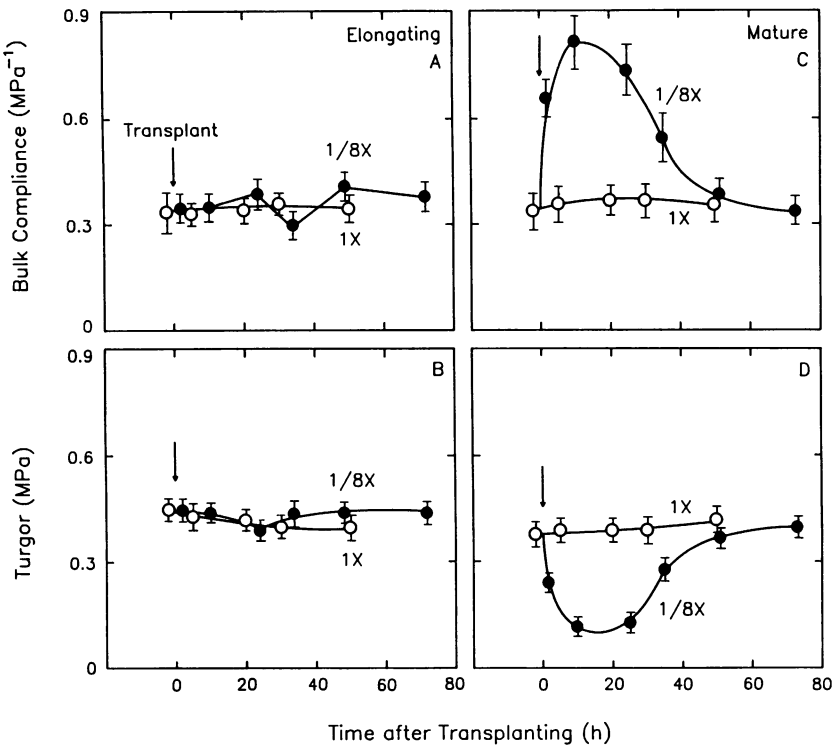


**Figure 7.** Bulk compliance (A and C) and turgor (B and D) of cortical cells in the elongating region (A and B) and mature region (C and D) of stems of intact soybean seedlings measured with the pressure probe. (○) represent plants grown in 1× vermiculite and (●) represent plants grown in 1/8× vermiculite. *Vertical bars* indicate 95% confidence intervals (Student's *t*-distribution).

intact plants were exposed to a root medium having low water content. In the present work, we show that the extensibility change can be detected with a simple unidirectional pull on the stem of the intact plant using an extensiometer and that the conductance change can be detected in individual cells of similarly intact plants with a pressure probe. The kinetics of the changes were similar with all the methods, and each showed the same moderate recovery at the end of the experiment. These results support the conclusion (27) that wall extensibility and tissue conductance decreased at low $\psi_w$ and eventually regulated growth when water supplies were limited. The effects were not immediate because the primary events appeared to be physical, and biochemical alterations followed. Eventually, most of the physical changes recovered and only the extensibility and conductance remained low enough to be regulating.

It is important to note that the extensibilities were virtually the same when measured with the psychrometer (Fig. 6C in Nonami and Boyer [27]) and extensiometer (Fig. 4A). Moreover, the extensibilities of killed samples were similar to those of living tissues (*cf.* Figs. 4A and 6A). Because the killed samples could not have been engaged in wall biosynthesis, these results indicate not only that the psychrometer and extensiometer measured the same tissue extensibility but also that the extensibility was a physical property of the wall rather than a reflection of the rate of wall biosynthesis. Thus, the cell walls in the growth-affected tissue must have been physically different from those in the control tissue.

It is possible that enzyme activity remained after freezing and thawing the tissue and that hydrolysis of wall constituents took place even though biosynthesis was disrupted. The measurements were made rapidly to minimize this possibility, and continued measurements showed little change in tissue characteristics over long times, suggesting that residual enzyme activity was low.

Others reported low wall extensibilities in plants subjected to low $\psi_w$ (8, 14, 15, 22, 30) or in cultured cells acclimated to low $\psi_w$ (7), but the observations generally required days (8, 14, 22, 30) during which extensibilities could change. Methods involving exposure to osmotica (7, 9) are faster but have the problem that solutes can cross cell membranes and, if there is a low reflection coefficient, can cause the solute content of the cells to be overestimated. This leads to erroneous estimates of extensibility. Stress relaxation techniques (10, 11, 37) employing Instron type measurements avoid this error but can only be used with killed tissue segments and are often variable.

The extensiometer method of Kutschera and Schopfer (19, 20) was not subject to these problems and should be applicable to intact plants. In the present work, we adapted their method to intact growing plants and found that, when expressed in the appropriate physical units, absolute extensibilities could be obtained. Moreover, the measurements were rapid and reproducible. Wall behavior conformed to that for an ideal viscoelastic polymer, *i.e.* the elastic and plastic components of wall extension were additive according to the superposition principle, and both responded linearly to the applied force, as expected if elastic extension was Hookian and plastic extension was Newtonian. No evidence of a yield threshold was observed because turgor already placed the stress on the wall at or above the yield threshold.

The method required the length of the elongating region to be known. Although Paolillo (29) claimed that the region shortened at low $\psi_w$, we observed no evidence of this effect (24). The reasons for this discrepancy are unknown, although

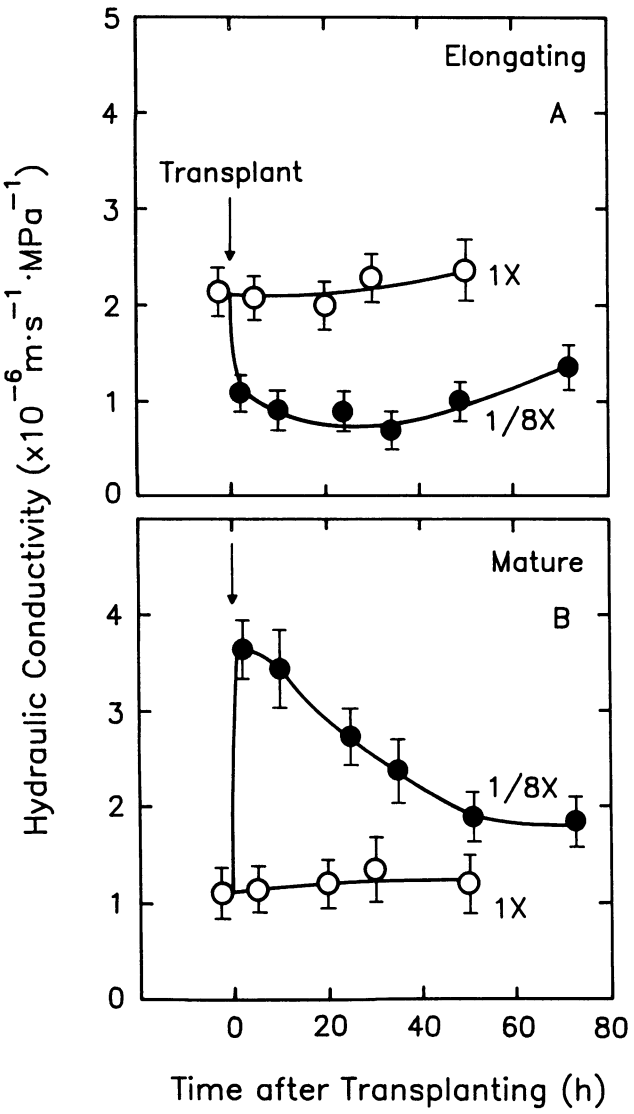


**Figure 8.** Hydraulic conductivity of cortical cells in the elongating region (A) and the mature region (B) of stems of intact soybean plants measured with the pressure probe. (○) represent plants grown in 1× vermiculite and (●) represent plants grown in 1/8× vermiculite. *Vertical bars* indicate 95% confidence intervals (Student's *t*-distribution).

it is noteworthy that his plants were subject to transplant shock that decreased growth rate and final cell lengths. Our plants did not experience transplant shock (see data of Meyer and Boyer [24] and Nonami and Boyer [27] for cell profiles and growth rates).

The alterations in wall physical properties detected by the extensiometer method were accompanied by changes in the hydraulic conductivity of the cells for water. Whether the conductivity was altered because of changes in the walls or plasmalemma or rates of cyclosis cannot be determined from the present work but, for the tissue as a whole, the conductance was diminished sufficiently to contribute to the growth limitation (27).

Although the relative changes in conductance were similar at the tissue and cell levels, the numerical values for tissue conductance (Fig. 6B of Nonami and Boyer [27]) and cell conductivity (Fig. 8A) differed because of the influence of tissue geometry and cell types. It is possible to predict tissue characteristics from cell data when geometrical features of the tissue are taken into account (25, 31–33), but this was not done in the present work because cell properties were measured only in the cortical cells and did not include the small noncortical cells enclosing the xylem that could have restricted water flow (see Steudle and Boyer [33], for photomicrograph of this tissue). Others (12, 13) observed hydraulic conductivities similar to those we report, but Cosgrove and Cleland (12) extrapolated these values to those for the entire stem which may be incorrect. It was recently reported (26) that turgor could be lost transiently in undifferentiated small cells next to the xylem without transmission to the cortical cells. This implies that water flow in the tissue was more restricted than would be indicated from measurements in cortical cells alone.

The conductivity changes in the elongating tissues did not involve changes in cell wall elasticity, which was constant after transplanting even though marked changes in conductivity had taken place. Moreover, the bulk compliance did not differ appreciably between elongating and mature tissue unless the turgor differed. This is further evidence that the elastic and plastic properties were independent of each other and that the superposition principle holds for cell walls.

We conclude that the plastic properties of cell walls and the conductivities of cell membranes were changed in elongating stem tissues when plants were exposed to growth-inhibiting $\psi_w$ around the roots for several hours, but the elastic properties of the walls were independent of these changes. The results indicate that the psychrometer, extensiometer, and pressure probe give similar results and are useful methods for monitoring these parameters in intact plants.

## ACKNOWLEDGMENT

We are indebted to Dr. Paul R. Austin for stimulating our interest in polymer physics.

## LITERATURE CITED

1. **Alfrey T** (1948) Mechanical Behavior of High Polymers. Interscience Publishers, New York
2. **Bensen RJ, Boyer JS, Mullet JE** (1988) Water deficit induced changes in abscisic acid content, growth rates, polysomes and translatable RNA in the elongating region of etiolated soybean hypocotyls. Plant Physiol **88:** 289–294
3. **Boyer JS** (1970) Leaf enlargement and metabolic rates in corn, soybean, and sunflower at various leaf water potentials. Plant Physiol **46:** 233–235.
4. **Boyer JS, Cavalieri AJ, Schulze E-D** (1985) Control of the rate of cell enlargement: excision, wall relaxation, and growth-induced water potentials. Planta **163:** 527–543
5. **Boyer JS, Knipling EB** (1965) Isopiestic technique for measuring leaf water potentials with a thermocouple psychrometer. Proc Natl Acad Sci USA **54:** 1044–1051
6. **Bozarth CS, Mullet JE, Boyer JS** (1987) Cell wall proteins at low water potentials. Plant Physiol **85:** 261–267
7. **Bressan RA, Handa AK, Handa S, Hasegawa PM** (1982) Growth and water relations of cultured tomato cells after adjustment to low external water potentials. Plant Physiol **70:** 1303–1309
8. **Bunce JA** (1977) Leaf elongation in relation to leaf water potential in soybean. J Exp Bot **28:** 156–161

9. **Cleland R** (1959) Effect of osmotic concentration on auxin-action and on irreversible and reversible expansion of the *Avena* coleoptile. Physiol Plant **12:** 809–825
10. **Cleland R** (1967) Extensibility of isolated cell walls: measurement and changes during cell elongation. Planta **74:** 197–209
11. **Cleland RE** (1984) The instron technique as a measure of immediate-past wall extensibility. Planta **160:** 514–520
12. **Cosgrove DJ, Cleland RE** (1983) Osmotic properties of pea internodes in relation to growth and auxin action. Plant Physiol **72:** 332–338
13. **Cosgrove DJ, Steudle E** (1981) Water relations of growing pea epicotyl segments. Planta **153:** 343–350
14. **Cutler JM, Shahan KW, Steponkus PL** (1980) Influence of water deficits and osmotic adjustment on leaf elongation in rice. Crop Sci **20:** 314–318
15. **Davies WJ, Van Volkenburgh E** (1983) The influence of water deficit on the factors controlling the daily pattern of growth of *Phaseolus* trifoliates. J Exp Bot **34:** 987–999
16. **Feynman RP, Leighton RB, Sands M** (1964) Lectures on Physics, Vol II. Addison-Wesley, Reading, MA, p 42-13
17. **Green PB, Cummins WR** (1974) Growth rate and turgor pressure. Auxin effect studied with an automated apparatus for single coleoptiles. Plant Physiol **54:** 863–869
18. **Hüsken D, Steudle E, Zimmermann U** (1978) Pressure probe technique for measuring water relations of cells in higher plants. Plant Physiol **61:** 158–163
19. **Kutschera U, Schopfer P** (1986) Effect of auxin and abscisic acid on cell wall extensibility in maize coleoptiles. Planta **167:** 527–535
20. **Kutschera U, Schopfer P** (1986) In-vivo measurement of cell-wall extensibility in maize coleoptiles: effects of auxin and abscisic acid. Planta **169:** 437–442
21. **Mason HS, Mullet JE, Boyer JS** (1988) Polysomes, messenger RNA and growth in soybean stems during development and water deficit. Plant Physiol **86:** 725–733
22. **Matthews MA, Van Volkenburgh E, Boyer JS** (1984) Acclimation of leaf growth to low water potentials in sunflower. Plant Cell Environ **7:** 199–206
23. **Matyssek R, Maruyama S, Boyer JS** (1988) Rapid wall relaxation in elongating tissues. Plant Physiol **86:** 1163–1167
24. **Meyer RF, Boyer JS** (1972) Sensitivity of cell division and cell elongation to low water potentials in soybean hypocotyls. Planta **108:** 77–87
25. **Molz FJ, Boyer JS** (1978) Growth-induced water potential in plant cells and tissues. Plant Physiol **62:** 423–429
26. **Nonami H, Boyer JS** (1989) Turgor and growth at low water potentials. Plant Physiol **89:** 798–804
27. **Nonami H, Boyer JS** (1990) Primary events regulating stem growth at low water potentials. Plant Physiol **93:** 1601–1609
28. **Nonami H, Boyer JS, Steudle E** (1987) Pressure probe and isopiestic psychrometer measure similar turgor. Plant Physiol **83:** 1601–1609
29. **Paolillo DJ Jr** (1989) Cell and axis elongation in etiolated soybean seedlings are altered by moisture stress. Bot Gaz **150:** 101–107
30. **Radin JW, Boyer JS** (1982) Control of leaf expansion by nitrogen nutrition in sunflower plants: role of hydraulic conductivity and turgor. Plant Physiol **69:** 771–775
31. **Silk WK, Wagner KK** (1980) Growth-sustaining water potential distributions in the primary corn root. Plant Physiol **66:** 859–863
32. **Steudle E, Jeschke WD** (1983) Water transport in barley roots. Planta **158:** 237–248
33. **Steudle E, Boyer JS** (1985) Hydraulic resistance to water flow in growing hypocotyl of soybean measured by a new pressure-perfusion technique. Planta **164:** 189–200
34. **Steudle E, Zimmermann U, Lüttge U** (1977) Effect of turgor pressure and cell size on the wall elasticity of plant cells. Plant Physiol **59:** 285–289
35. **Van Volkenburgh E, Boyer JS** (1985) Inhibitory effects of water deficit on maize leaf elongation. Plant Physiol **77:** 190–194
36. **Wainwright SA, Biggs WD, Currey JD, Gosline JM** (1976) Mechanical Design in Organisms. Edward Arnold, London
37. **Yamamoto R, Shinozaki K, Masuda Y** (1970) Stress-relaxation properties of plant cell walls with special reference to auxin action. Plant Cell Physiol **11:** 947–956